







## NDRG1 in Aggressive Breast Cancer Progression and Brain Metastasis

Emilly S. Villodre, PhD,<sup>1,2</sup> Xiaoding Hu, PhD <sup>1,2</sup> Bedrich L. Eckhardt, PhD,<sup>1,2,3</sup> Richard Larson, MS,<sup>2,4</sup> Lei Huo, MD, PhD <sup>2,5</sup> Ester C. Yoon, MD,<sup>5</sup> Yun Gong, MD,<sup>2,5</sup> Juhee Song, PhD <sup>6</sup> Shuying Liu, MD, PhD,<sup>1</sup> Naoto T. Ueno, MD, PhD <sup>1,2</sup> Savitri Krishnamurthy, MD,<sup>2,5</sup> Stefan Pusch, PhD <sup>7,8</sup> Debu Tripathy, MD <sup>1,2</sup> Wendy A. Woodward, MD, PhD,<sup>2,4</sup> Bisrat G. Debeb, DVM, PhD<sup>1,2,\*</sup>

<sup>1</sup>Department of Breast Medical Oncology, The University of Texas MD Anderson Cancer Center, Houston, TX, USA; <sup>2</sup>MD Anderson Morgan Welch Inflammatory Breast Cancer Clinic and Research Program, The University of Texas MD Anderson Cancer Center, Houston, TX, USA; <sup>3</sup>Olivia Newton-John Cancer Research Institute, School of Cancer Medicine, La Trobe University, Bundoora, Victoria, Australia; <sup>4</sup>Department of Radiation Oncology, The University of Texas MD Anderson Cancer Center, Houston, TX, USA; <sup>5</sup>Department of Pathology, The University of Texas MD Anderson Cancer Center, Houston, TX, USA; <sup>6</sup>Department of Biostatistics, The University of Texas MD Anderson Cancer Center, Houston, TX, USA; <sup>7</sup>German Cancer Consortium Clinical Cooperation Unit Neuropathology, German Cancer Research Center, Heidelberg, Germany; and <sup>8</sup>Department of Neuropathology, Heidelberg University Medical Center, Heidelberg, Germany

\*Correspondence to: Bisrat G. Debeb, DVM, PhD, Department of Breast Medical Oncology, Section of Translational Breast Cancer Research, The Morgan Welch Inflammatory Breast Cancer Research Program and Clinic, The University of Texas MD Anderson Cancer Center, 6565 MD Anderson Blvd, Houston, TX 77030, USA (e-mail: bgdebeb@mdanderson.org).

### Abstract

**Background:** N-Myc downstream regulated gene 1 (NDRG1) suppresses metastasis in many human malignancies, including breast cancer, yet has been associated with worse survival in patients with inflammatory breast cancer. The role of NDRG1 in the pathobiology of aggressive breast cancers remains elusive. **Methods:** To study the role of NDRG1 in tumor growth and brain metastasis in vivo, we transplanted cells into cleared mammary fat pads or injected them in tail veins of SCID/Beige mice (n = 7-10 per group). NDRG1 protein expression in patient breast tumors (n = 216) was assessed by immunohistochemical staining. Kaplan-Meier method with 2-sided log-rank test was used to analyze the associations between NDRG1 and time-to-event outcomes. A multivariable Cox regression model was used to determine independent prognostic factors. All statistical tests were 2-sided. **Results:** We generated new sublines that exhibited a distinct propensity to metastasize to the brain. NDRG1-high-expressing cells produced more prevalent brain metastases (100% vs 44.4% for NDRG1-low sublines, P = .01, Fisher's exact test), greater tumor burden, and reduced survival in mice. In aggressive breast cancer cell lines, silencing NDRG1 led to reduced migration, invasion, and tumor-initiating cell subpopulations. In xenograft models, depleting NDRG1 inhibited primary tumor growth and brain metastasis. In patient breast tumors, NDRG1 was associated with aggressiveness: NDRG1-high expression was also associated with shorter overall survival (hazard ratio [HR] = 2.27, 95% confidence interval [95% CI] = 1.20 to 4.29, P = .009) and breast cancer-specific survival (HR = 2.19, 95% CI = 1.07 to 4.48, P = .03). Multivariable analysis showed NDRG1 to be an independent predictor of overall survival (HR = 2.17, 95% CI = 1.10 to 4.30, P = .03) and breast cancer-specific survival rates (HR = 2.27, 95% CI = 1.05 to 4.92, P = .04). **Conclusions:** We demonstrated that NDRG1 drives tumor progression and brain metastasis in aggressive breast cancers and that NDRG1-high expression correlates with worse clinical outcomes, suggesting that NDRG1 may serve as a therapeutic target and prognostic biomarker in aggressive breast cancers.

Brain metastasis is a common manifestation of systemic malignancies, including lung, breast, and skin cancers (1,2). Patients with advanced breast cancer have an estimated 18%-30% incidence of brain metastasis and a poor prognosis, with median survival intervals of only 5 to 6 months (3-5). Patients with aggressive HER2+ or triple-negative breast cancer (TNBC) subtypes are at greater risk of brain metastasis (6,7). Current treatment

options for brain metastases offer limited disease control, underscoring the urgent need to develop better therapeutic approaches.

Understanding the pathobiology of brain metastasis, identifying targets, and developing effective therapies have been hampered by the scarcity of experimental models. We recently developed preclinical mouse models of brain metastasis via

tail-vein injection of HER2+ or TNBC breast cancer cell lines (8,9) and used these models to identify key regulators of metastasis to the brain and to test potential therapeutic strategies (8,10-12). In the current study, we generated new sublines from an aggressive breast cancer cell line that display distinct morphology and propensity for brain metastasis and express different levels of the stress response protein N-Myc downstream regulated gene 1 (NDRG1). The role of NDRG1 in human cancer remains controversial. In pancreatic, ovarian, and colorectal cancer cells, NDRG1 acts as a metastasis suppressor; on the other hand, NDRG1 has been described as a biomarker of metastasis, cancer recurrence, and poor prognosis in hepatocellular carcinoma, bladder, and cervical cancers (13-22). As for breast cancer, most studies show a tumor suppressor function but others a metastasis-promoter function (2-26). Nevertheless, the role of NDRG1 in promoting tumor growth and metastatic tumor phenotype in aggressive breast cancers remains unclear.

Here, we demonstrate that NDRG1 promotes invasion and enrichment of tumor-initiating cell populations in vitro and tumor progression and brain metastasis in mouse models of aggressive breast cancer. In tumors from breast cancer patients, NDRG1-high expression was linked with aggressive tumor characteristics and independently predicted poor survival outcomes.

## Methods

### Mouse Studies

All mouse experiments were preapproved by the Institutional Animal Care and Use Committee of MD Anderson Cancer Center. SCID/Beige mice were purchased from Harlan Laboratories (Indianapolis, IN, USA). Metastatic colonization was achieved by tail-vein injection of breast cancer cells into 4- to 6-week-old female SCID/Beige mice. For xenograft tumor growth studies, cells were injected into cleared mammary fat pads of SCID/Beige mice. Methods for measuring, resecting, and imaging tumors are given in the [Supplementary Methods](#) (available online).

### Tissue Microarrays (TMAs)

Tumor samples from patients with invasive breast cancer ( $n = 216$ ) seen at MD Anderson were immunostained for NDRG1 in a TMA generated by L.H. NDRG1 staining was scored and interpreted by 2 pathologists (L.H., E.C.Y.). Details are given in the [Supplementary Methods](#) (available online).

### Statistical Analysis

All in vitro experimental analyses were repeated at least 3 times, and data are represented in graphs as means with error bars indicating SD. Statistical significance was determined with Student's *t* tests unless otherwise specified. All statistical tests were 2-sided. For primary tumor growth, we transplanted NDRG1 control and NDRG1-silenced SUM149 and MDA-IBC3 cells into cleared mammary fat pads of SCID/Beige mice ( $n = 7-10$  per group). For brain metastasis studies, we injected NDRG1 control and NDRG1-silenced MDA-IBC3 cells via tail vein of SCID/Beige mice ( $n = 9-10$  per group). Fisher's exact test was used to compare the incidence of brain metastatic colonization between sublines or NDRG1 control and silenced MDA-IBC3 cell line. For TMA immunohistochemical staining, patient breast tumors ( $n = 216$ ) were stratified by NDRG1 value (low [ $\leq$  median]

vs high [ $>$  median]) and compared between groups. The association between NDRG1 and time-to-event outcomes was analyzed with the Kaplan-Meier method and 2-sided log-rank test. A multivariable Cox regression model was used to determine independent prognostic factors. SAS 9.4 (SAS Institute Inc, Cary, NC, USA) was used for data analysis. *P* values less than .05 indicated statistically significant differences. Further details are given in the [Supplementary Methods](#) (available online).

## Results

### Novel MDA-IBC3 Breast Cancer Derivatives With Distinct Propensity to Develop Brain Metastasis

We derived new sublines of MDA-IBC3 (designated MDA-IBC3.1 and MDA-IBC3.2) that display distinct morphology in cell culture ([Figure 1, A](#)). Notably, these sublines exhibit a distinct propensity to metastasize to the brain on tail-vein injection into mice. Mice injected with MDA-IBC3.1 cells were less likely to form brain metastases than MDA-IBC3.2 (44.4% vs 100%,  $P = .01$ , 2-sided Fisher's exact test; [Figure 1, B](#)), with smaller metastatic burden ([Figure 1, C](#); [Supplementary Figure 1, A](#), available online), fewer brain metastases per mouse ([Supplementary Figure 1, B](#), available online), and longer latency as indicated in [Figure 1, D](#) (70% vs 11%,  $P = .02$ , at 15 weeks). Moreover, MDA-IBC3.2-injected mice had worse brain metastasis-free survival (BrMFS) (hazard ratio [HR] = 4.88, 95% confidence interval [95% CI] = 1.61 to 14.75,  $P < .001$ ; [Figure 1, E](#)) and overall survival (OS) (HR = 6.83, 95% CI = 2.04 to 22.84,  $P = .002$ ; [Figure 1, F](#)). Compared with the parental MDA-IBC3 cells, MDA-IBC3.1 cells showed no difference in the incidence of brain metastasis, OS, and BrMFS ([Supplementary Figure 1, C-E](#), available online), but MDA-IBC3.1 cells led to fewer brain metastases per mouse ([Supplementary Figure 1, B](#), available online). For the MDA-IBC3.2 subline, no difference was found in incidence of brain metastasis vs parental cells ([Supplementary Figure 1, C](#), available online), but MDA-IBC3.2-injected mice had worse BrMFS and OS than parental cell-injected mice ([Supplementary Figure 1, D and E](#), available online). Hematoxylin and eosin staining of brain metastases from the 2 sublines showed similar histologic characteristics ([Supplementary Figure 1, F](#)). We previously showed that tail-vein-injected MDA-IBC3 cells preferentially metastasize to the brain vs other organs (8). Similarly, we observed quite low rates of lung metastasis (0%-20%) after tail-vein injection of the new sublines. Our findings show that the MDA-IBC3.2 subline has an enhanced propensity to metastasize to the brain relative to MDA-IBC3.1.

Next, to identify proteins associated with aggressive brain metastasis, we used reverse-phase protein array proteomic profiling to compare protein expression patterns in the 2 sublines. We identified several proteins that were differentially expressed, with phosphorylated NDRG1 (NDRG1\_pT346) being the top downregulated protein in the less aggressive MDA-IBC3.1 subline ([Figure 1, G](#); [Supplementary Table 1](#), available online). We confirmed reduced expression of NDRG1 and NDRG1\_pT346 proteins in MDA-IBC3.1 cells by immunoblotting ([Figure 1, I](#)).

Next, we analyzed independent cohorts of patients whose datasets included information on metastases and primary tumors. NDRG1 was expressed at higher levels in brain metastases than in matched primary tumors ( $P = .02$ ; [Figure 1, J](#)) or non-matched primary tumors (mean [SD], 617.2 [801.5] vs 216.3 [184.9],  $P = .02$ ; [Figure 1, K](#)). Moreover, patients with NDRG1-

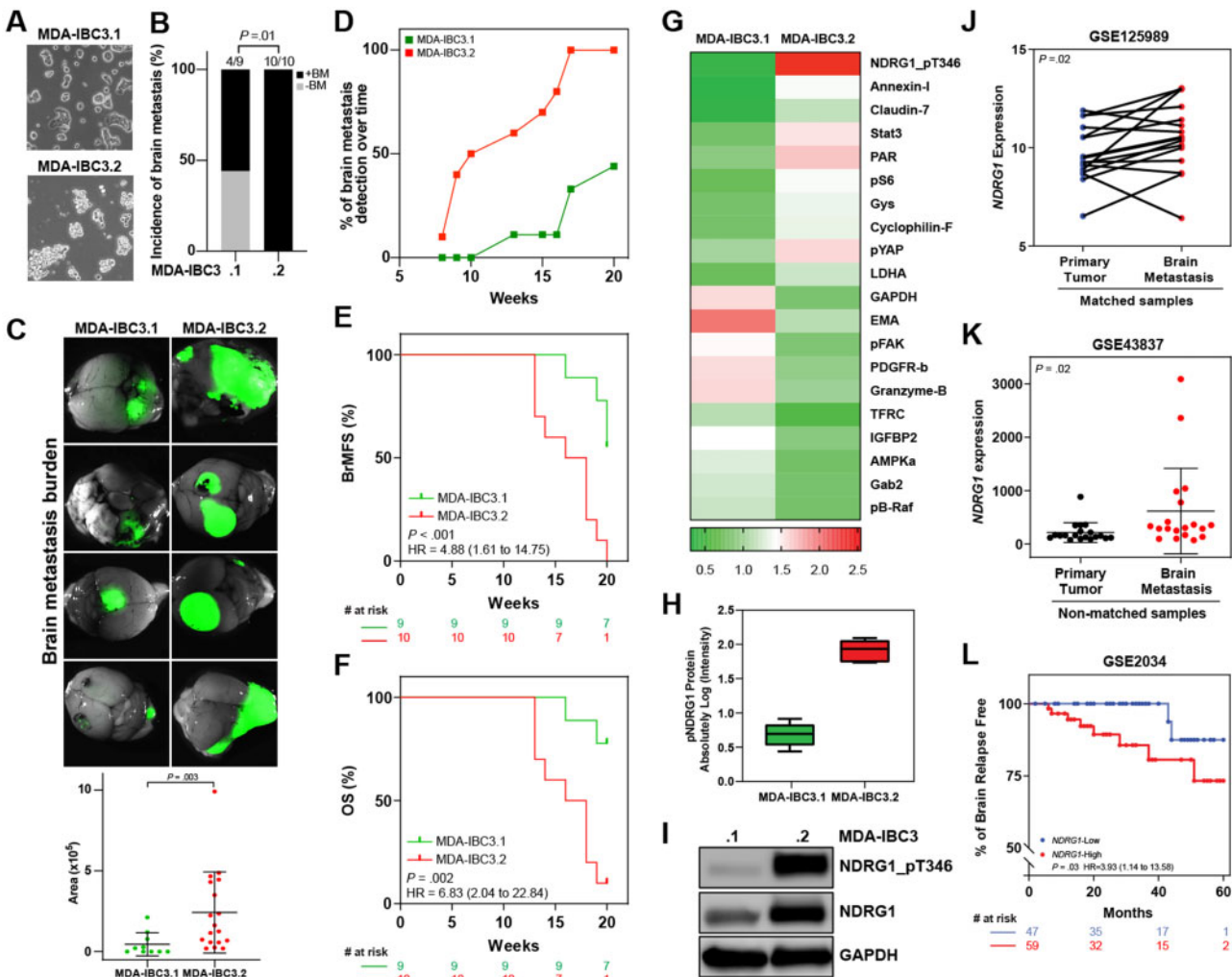


**Figure 1.** Novel MDA-IBC3 breast cancer sublines with different propensities for brain metastasis. **A)** The novel MDA-IBC3 sublines show distinct morphology in cell culture. **B)** Incidence of brain metastasis in mice injected with MDA-IBC3.1 and MDA-IBC3.2 sublines ( $P$  value from 2-sided Fisher's exact test). **C)** Representative images of brain metastasis generated after tail-vein injection of MDA-IBC3.1 and MDA-IBC3.2 sublines, with quantification of brain metastasis burden. The horizontal lines indicate means and error bars indicate SD.  $P$  value from 2-sided Mann-Whitney test. **D)** Time to detect brain metastases (BM) was measured by detection of luciferase signal. Kaplan-Meier estimates of brain metastasis-free survival (BrMFS) **E)** and overall survival (OS) of MDA-IBC3.1 ( $n=9$ ) and MDA-IBC3.2 ( $n=10$ ) **F)**.  $P$  values from 2-sided log-rank tests and the hazard ratio (HR) with 95% confidence interval are shown for each graph. **G)** Heatmap from reverse-phase protein array analysis shows top differentially expressed proteins (fold change) in the MDA-IBC3.1 and MDA-IBC3.2 sublines. Data presented as means of 6 replicates for each sample. **H)** Reverse-phase protein array findings for phosphorylated NDRG1 (NDRG1\_pT346). Horizontal lines indicate means and ranges. **I)** Immunoblotting analysis of expression of total NDRG1 and NDRG1\_pT346 for the 2 sublines. GAPDH was used as internal control. Analysis of publicly available datasets for NDRG1 expression in matched primary tumor and brain metastasis (GSE125989,  $n=16$ ) **J)** and in unmatched samples (GSE43837,  $n=19$ ) **K)**. **J)**  $P$  values from 2-sided Wilcoxon tests; **K)** horizontal lines indicate means and error bars indicate SD.  $P$  value from 2-sided Mann-Whitney test. **L)** Percentage of patients free of brain relapse stratified by NDRG1 expression [GSE2034; NDRG1-low ( $n=47$ ); NDRG1-high ( $n=60$ )].  $P$  values from 2-sided log-rank test and the hazard ratio with 95% confidence interval are shown. RPPA = reverse phase protein array.

high-expressing tumors had reduced brain metastasis relapse-free survival vs NDRG1-low tumors (HR = 3.93, 95% CI = 1.14 to 13.58,  $P = .03$ ; **Figure 1, L**), leading us to propose that NDRG1 functions to enhance brain metastasis in aggressive breast cancers.

### Association Between NDRG1 Expression and Breast Cancer Aggressiveness Features

We next analyzed several independent, publicly available datasets of breast cancer patients to examine associations of NDRG1 expression with clinicopathological variables and outcomes. NDRG1 was expressed at higher levels in tumor tissue than in normal breast (**Figure 2, A**) and estrogen receptor (ER)-negative

tumors relative to ER-positive tumors ( $P < .001$ ; **Figure 2, B**). We also found higher NDRG1 expression in more aggressive HER2+ and basal-like molecular subtypes than in luminal subtypes ( $P < .001$ ; **Figure 2, C**), in TNBC (ER<sup>-</sup>/PR<sup>-</sup>/HER2<sup>+</sup>) vs non-TNBC ( $P < .001$ ; **Figure 2, D**), and in high-grade breast tumors ( $P < .001$ ; **Figure 2, E**).

We assessed possible associations between tumor NDRG1 expression and survival outcomes. NDRG1-high expression was found to correlate with reduced OS (**Figure 2, F**; **Supplementary Figure 2, A**, available online). NDRG1 expression was higher in patients who presented with metastasis (**Figure 2, G**), and NDRG1-high expression was associated with worse metastasis-free survival (**Figure 2, H**; **Supplementary Figure 2, B**, available online). Notably, NDRG1, located on chromosome 8q24, was

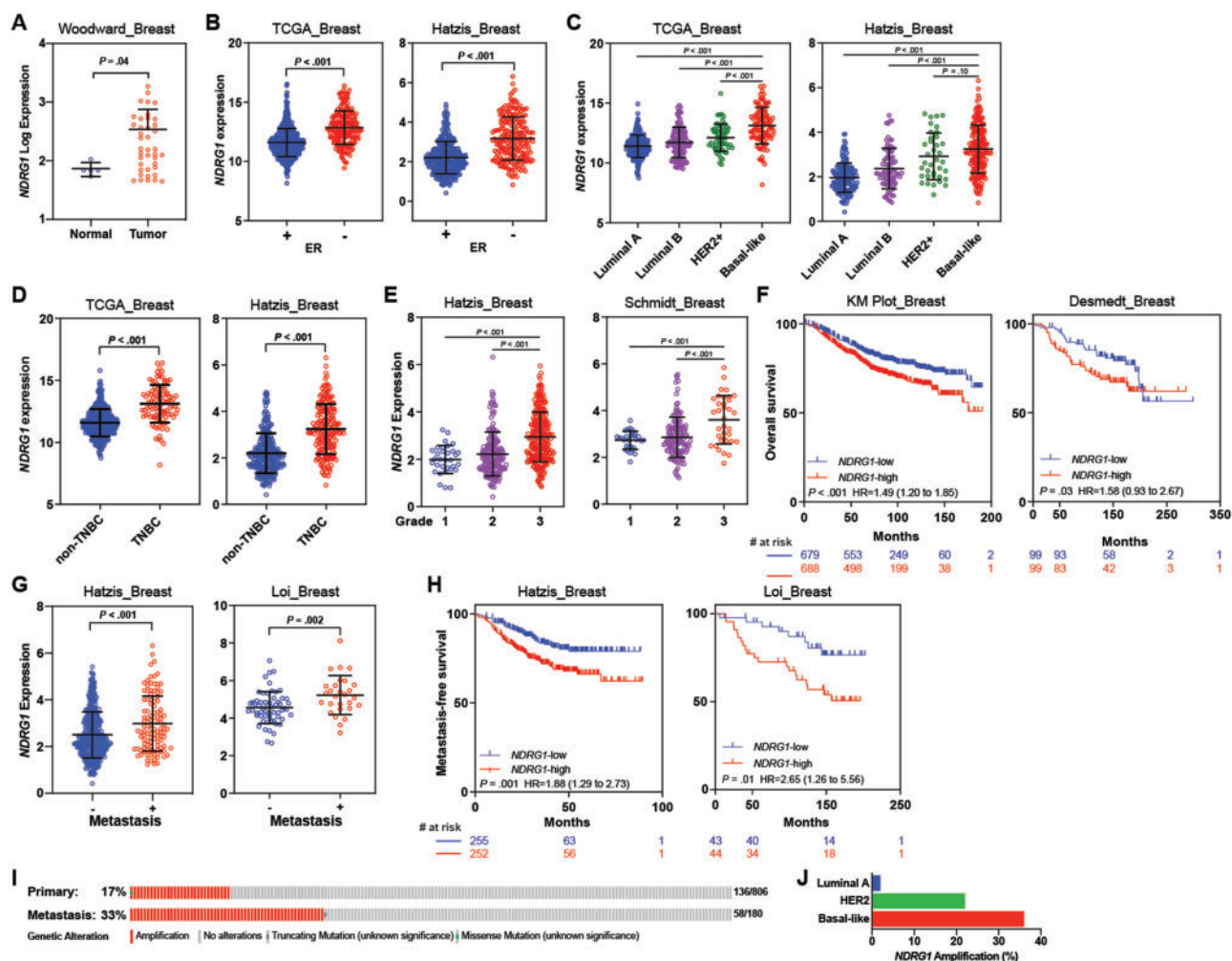


**Figure 2.** Analysis of *NDRG1* expression in breast cancer and its correlation with survival outcome. **A)** *NDRG1* expression in breast tumor samples and in normal tissue (Woodward—GSE45581). *NDRG1* expression according to **B)** estrogen receptor (ER) status, **C)** breast cancer molecular subtype, **D)** triple-negative breast cancer (TNBC) vs non-TNBC status, and **E)** grade in tumor samples from patients with breast cancer. **F)** Kaplan-Meier (KM) curve estimates of overall survival by *NDRG1* status using KM Plot [*NDRG1*-low ( $n = 701$ ); *NDRG1*-high ( $n = 701$ )] and Desmedt [*NDRG1*-low ( $n = 99$ ); *NDRG1*-high ( $n = 99$ )] datasets. **G)** *NDRG1* expression by metastasis status. **H)** KM estimates of metastasis-free survival using Hatzis dataset [*NDRG1*-low ( $n = 255$ ); *NDRG1*-high ( $n = 253$ )] and Loi dataset [*NDRG1*-low ( $n = 43$ ); *NDRG1*-high ( $n = 44$ )]. Independent cohorts were used to analyze *NDRG1* median expression and survival outcomes. Horizontal lines indicate mean and error bars indicate SD. *P* values were calculated with 2-sided Mann-Whitney tests (**A–E**, **G**) and 2-sided log-rank tests, and the hazard ratio (HR) with 95% confidence interval (95% CI) is shown (**F**, **H**). **I)** *NDRG1* amplification analysis in primary tumors (from The Cancer Genome Atlas [TCGA]) and metastatic breast cancer tumors (from the Metastatic breast cancer project dataset—CBioPortal). **J)** *NDRG1* amplification in primary breast cancer by molecular subtype (data from TCGA). ER = estrogen receptor.

highly amplified in patients with metastatic and basal-like breast tumors. *NDRG1* was amplified in 33% of metastatic breast tumors in the Metastatic Breast Cancer dataset vs 17% of primary breast tumors from the TCGA invasive breast cancer dataset (27) (Figure 2, I); further stratification of *NDRG1* amplification by molecular subtype of the invasive breast cancer dataset revealed increased *NDRG1* amplification in the basal-like subtype (36%), followed by the HER2+ (25%) and Luminal A (2.8%) subtypes, indicating that *NDRG1* is linked to tumor aggressiveness features (Figure 2, J). Further, our TCGA data analysis shows that increased DNA copy number through amplification and gain of the *NDRG1* gene was associated with increased mRNA ( $P < .001$ ) and protein ( $P < .001$ ) expression levels (Supplementary Figure 2, C, available online) relative to nonamplified tumors.

We further validated these observations by immunostaining a TMA consisting of several breast cancer patient-derived xenograft (PDX) and mouse xenograft tumors (Supplementary Figure

3, A). We found cytoplasmic *NDRG1* protein expression to be heterogeneous (Supplementary Figure 3, B and C, available online). *NDRG1* score was higher in more aggressive ER-negative and TNBC tumors relative to ER+ (mean [SD], 83.42 [61.17] vs 21.25 [17.50],  $P = .05$ ) and non-TNBC tumors (mean [SD], 93.33 [59.66] vs 37.92 [46.54],  $P = .006$ , respectively; Supplementary Figure 3, D–F, available online). Collectively, our findings demonstrate that *NDRG1* was positively correlated with poor clinical outcomes and with molecular and pathological tumor traits commonly associated with aggressiveness.

### Effect of *NDRG1* Silencing on Invasion of Aggressive Breast Cancer Cells and Tumor-Initiating Cell Subpopulations

To investigate the role of *NDRG1* in aggressive breast cancers, we generated stable *NDRG1*-knockdown (KD) cell lines with

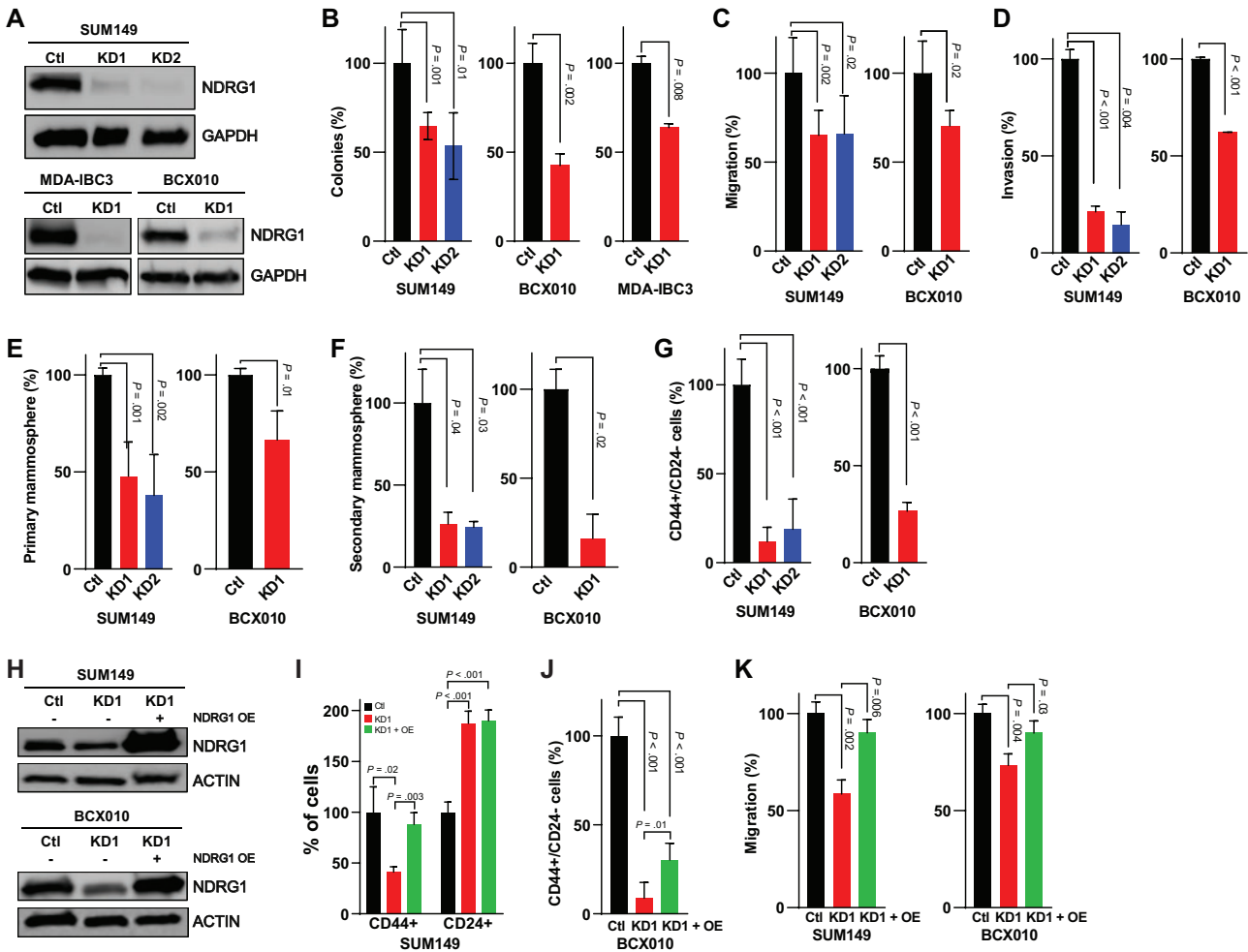


**Figure 3.** Effect of NDRG1 silencing on invasion and tumor-initiating cell subpopulations in aggressive breast cancer cells. **A)** Stable knockdown of NDRG1 in SUM149, MDA-IBC3, and BCX010 breast cancer cell lines by using lentiviral shRNA vectors confirmed by immunoblotting. **B)** Colony formation, **(C)** migration, and **(D)** invasion assay findings for NDRG1 control and NDRG1-silenced cells. **E)** Primary mammosphere formation and **(F)** secondary mammosphere formation in NDRG1 control and knockdown cells. **G)** Analysis of CD44<sup>+</sup>CD24<sup>-</sup> cells, a surrogate for tumor-initiating cells, in NDRG1 control and knockdown cells. **H)** Immunoblotting confirmed transient overexpression of NDRG1 in the NDRG1-silenced cells. **I)** Analysis of CD44<sup>+</sup> and CD24<sup>+</sup> subpopulations of SUM149 cells after overexpression of NDRG1 in depleted cells. **J)** CD44<sup>+</sup>CD24<sup>-</sup> cells of BCX010 cells after NDRG1 overexpression. **K)** Migration assay after NDRG1 overexpression in NDRG1-silenced cells. Bar graphs indicate means and error bars indicate SD, calculated after 3 independent experiments; P values from 2-sided t tests. Ctl = shRNA control; KD1 = knockdown variant 1; KD2 = knockdown variant 2; OE = overexpression.

lentiviral short hairpin (shRNA)s: 2 TNBC [SUM149, BCX010] and a HER2-positive [MDA-IBC3]. We confirmed KD of protein and mRNA expression by immunoblotting (Figure 3, A) and real-time polymerase chain reaction (RT-PCR, Supplementary Figure 4, A, available online). Silencing NDRG1 did not affect proliferation (Supplementary Figure 4, B–D, available online) but did reduce the capacity for colony formation (Figure 3, B). Because tumor cells from patients with aggressive breast cancers are migratory, carrying a high risk of metastatic disease, and are enriched in tumor-initiating cells, we investigated the effect of NDRG1 depletion on migration, invasion, and tumor-initiating cell subpopulations. Silencing NDRG1 expression reduced migration and invasion in SUM149 and BCX010 cells (Figure 3, C and D; Supplementary Figure 4, E and F, available online); knocking down NDRG1 also reduced primary and secondary mammospheres relative to control cells (Figure 3, E and F). We also found statistically significant reductions in CD44<sup>+</sup>CD24<sup>-</sup> cells in the NDRG1-depleted cells (mean [SD], SUM149 control [Ctl] = 100 [14.47], KD1 = 11.97 [7.91], KD2 = 18.85 [16.98]; BCX010

Ctl = 100 [6.62], KD1 = 26.58 [4.53],  $P < .001$ ; Figure 3, G; Supplementary Figure 4, G, available online). Overexpression of NDRG1 in depleted cells rescued the CD44<sup>+</sup>CD24<sup>-</sup> tumor-initiating cell population and the migration capacity (Figure 3, H–K; Supplementary Figure 4, H–J, available online). Of note, MDA-IBC3 cells are nonmigratory, noninvasive, and do not express a CD44<sup>+</sup>CD24<sup>-</sup> subpopulation in vitro, although they are tumorigenic in mouse xenografts. Taken together, our findings indicate that inhibition of NDRG1 in aggressive breast cancer cells suppresses traits associated with cancer cell aggressiveness.

### Impact of NDRG1 KD on Primary Tumor Growth and Brain Metastasis

To investigate the function of NDRG1 in tumor growth and progression, we transplanted control or NDRG1-KD SUM149 and MDA-IBC3 cells into the cleared mammary fat pads of immunocompromised SCID/Beige mice. Mice implanted with NDRG1-silenced SUM149 cells had statistically significantly smaller tumor

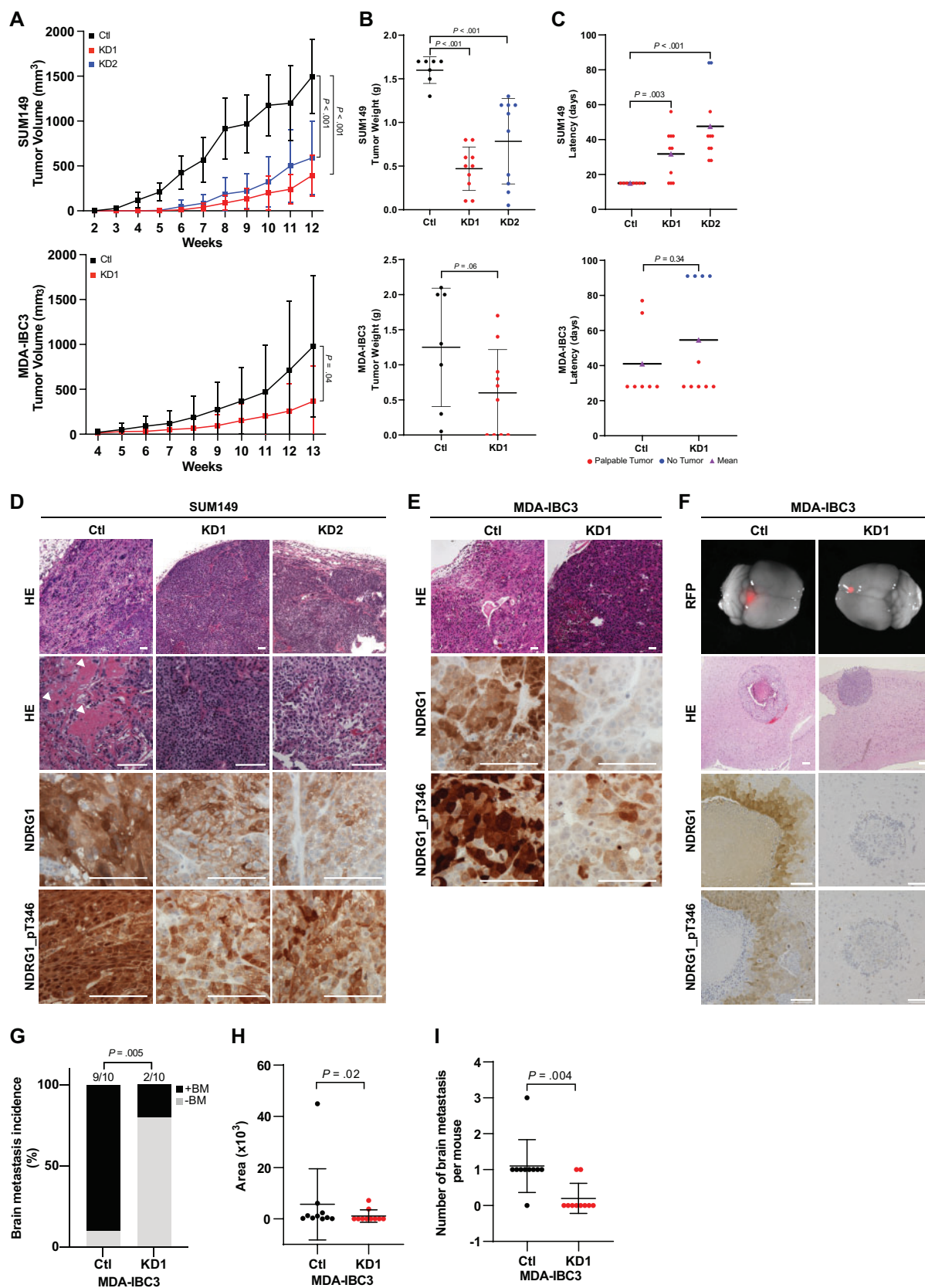


**Figure 4.** Impact of silencing NDRG1 on primary tumor growth and brain metastasis. **A**) Xenograft tumor volumes were measured weekly after transplantation of NDRG1 control (n = 7) and NDRG1-silenced (n = 10) SUM149 (mean [SD]: shRNA control [Ctl] = 1497 [410.9]; knockdown variant 1 [KD1] = 393.3 [229.5]; knockdown variant 2 [KD2] = 590.7 [408.5] mm<sup>3</sup>) or MDA-IBC3 (Ctl = 981.6 [787.8]; KD1 = 368.2 [395.1] mm<sup>3</sup>) cells. Graphs show mean and error bars indicate SD; P value from 2-sided t tests. **B**) Tumor weights after resection in SUM149 (Ctl = 1.6 [0.15]; KD1 = 0.47 [0.25]; KD2 = 0.78 [0.49] g) and MDA-IBC3 (Ctl = 1.3 [0.32]; KD1 = 0.6 [0.19] g) xenografts. Horizontal lines indicate mean and error bars indicate SD; P value from 2-sided t tests. **C**) Tumor latency (the time to initiation of tumor growth) in SUM149 (Ctl = 15 [0];

volumes (mean [SD], Ctl = 1497 [410.9], KD1 = 393.3 [229.5], KD2 = 590.7 [408.5],  $P < .001$ ; [Figure 4, A](#)) and weights (mean [SD], Ctl = 1.6 [0.15], KD1 = 0.47 [0.25], KD2 = 0.78 [0.49],  $P < .001$ ; [Figure 4, B](#)). The latency period was also longer in mice transplanted with NDRG1-silenced SUM149 cells relative to control-transplanted mice (mean [SD], 15 [0] vs 31.8 [14.46] days for Ctl vs KD1,  $P = .003$ ; 15 [0] vs 54.6 [20.82] days for KD2,  $P < .001$ ; [Figure 4, C](#)). Histologic examination showed that tumors from SUM149 control cells were invasive and poorly differentiated, with increased pleomorphic and metaplastic squamous cells and high levels of necrosis; although NDRG1-silenced SUM149 tumors were also poorly differentiated, they exhibited fewer metaplastic squamous cells and less necrosis ([Figure 4, D](#); [Supplementary Figure 5, A and B](#), available online). In previous studies, the presence of metaplastic squamous cells or necrosis has been associated with aggressive behavior and poor prognosis (28-30). Differences in necrosis were less evident for the MDA-IBC3-control and -KD transplanted tumors ([Figure 4, E](#); [Supplementary Figure 5, B](#), available online). Immunohistochemical staining of sections from SUM149 and MDA-IBC3 xenografts confirmed reduced expression of NDRG1 and NDRG1\_pT346 in tumors generated from NDRG1-silenced cells and showed the presence of highly proliferative Ki-67-positive cells, regardless of their NDRG1 expression status ([Figure 4, D and E](#); [Supplementary Figure 5, C and D](#), available online). We further confirmed the correlation between NDRG1 expression and increased necrosis in TMAs from breast cancer PDXs and xenografts, wherein NDRG1-high protein expression was in the peri-necrotic areas of tumors ([Supplementary Figure 5, E and F](#), available online).

To examine the role of NDRG1 in brain metastatic colonization, we injected red fluorescent protein (RFP)-labeled MDA-IBC3 NDRG1-control or -KD cells into the tail vein of SCID/Beige mice and examined the tumor incidence and tumor burden by fluorescent stereomicroscopy and histology. [Figure 4, F](#) shows representative images of brain metastasis and NDRG1/NDRG1\_pT346 expression. NDRG1 silencing statistically significantly inhibited the incidence of brain metastasis relative to control cells (10 of 10 Ctl mice vs 2 of 10 KD1 mice,  $P = .005$ , 2-sided Fisher's exact test; [Figure 4, G](#)). NDRG1 silencing also reduced the brain metastasis burden ([Figure 4, H](#)) and the number of brain metastases per mouse vs controls ([Figure 4, I](#)). Collectively, our in vivo findings implicate NDRG1 in tumor growth and brain metastasis in aggressive mouse models of breast cancer.

### NDRG1 Regulation of AKT Signaling in Aggressive Breast Cancer Cells

To identify potential pathways involved in NDRG1-mediated promotion of invasion and tumorigenesis, we first analyzed the TCGA proteomics dataset and found that NDRG1\_pT346 was associated with the mTOR-AKT signaling pathway ([Figure 5, A](#); [Supplementary Tables 2-4](#), available online). Moreover, gene set enrichment analysis of our proteomics data in the NDRG1-high

MDA-IBC3.2 subline showed enrichment of the PI3K-AKT-mTOR signaling pathway relative to the NDRG1-low MDA-IBC3.1 subline ([Supplementary Figure 6, A](#), available online). NDRG1 silencing in breast cancer cell lines showed reduction of phospho-AKT (AKT\_pS473, the bona fide mTORC2 activity read-out), whereas overexpression of NDRG1 in silenced cells rescued AKT\_pS473 expression ([Figure 5, B](#)). Consistently, immunostaining of sections from NDRG1-KD SUM149 tumor xenografts showed reduction in AKT\_pS473 levels ([Figure 5, C](#)), indicating that NDRG1 silencing impairs mTOR-AKT signaling. Treatment with AKT inhibitor MK2206 reduced the levels of AKT\_pS473, as expected; however, it did not affect the expression of NDRG1 or NDRG1\_pT346 ([Supplementary Figure 6, B](#), available online). Similarly, treating cells with PI3K inhibitors did not affect the expression of either NDRG1 or NDRG1\_pT346 ([Supplementary Figure 6, C](#), available online). However, AZD8055, a dual mTOR inhibitor, or BEZ235, a dual PI3K-mTOR inhibitor, reduced the levels of AKT\_pS473 and NDRG1\_pT346 at 1 h ([Supplementary Figure 6, D and F](#), available online) and at 24 hours ([Figure 5, D and F](#)) and reduced migration ([Figure 5, E and G](#); [Supplementary Figure 6, E and G](#), available online). Our results indicate that NDRG1 mediates its effects via phosphorylation of AKT in an mTOR-dependent but PI3K-independent mechanism ([Figure 5, H](#)).

### Prognostic Significance of NDRG1 in Patients With Breast Cancer

Given our finding from datasets that NDRG1 mRNA expression correlates with aggressiveness and poor outcome in patients with breast cancer ([Figure 2](#)), we immunostained NDRG1 on TMAs from 216 patients with breast cancer who had been treated at MD Anderson. The median follow-up time was 73 months. A representative image of the immunohistochemical staining for NDRG1 protein is shown in [Figure 6, A](#). NDRG1 was grouped as NDRG1-low ( $\leq$  the median) or NDRG1-high ( $>$  the median) based on the H-score. [Table 1](#) summarizes clinicopathological patient characteristics stratified by NDRG1 expression status. NDRG1 expression, pathological stage, tumor grade, hormone receptor status, ER status, progesterone receptor status, and TNBC status were associated with OS and breast cancer-specific survival (BCSS) ([Table 2](#)). NDRG1-high levels also were positively associated with ER-negative status, TNBC status, and high-grade tumors ([Figure 6, B-D](#)). NDRG1-high expression was also associated with shorter OS (HR = 2.27, 95% CI = 1.20 to 4.29,  $P = .009$ ) and BCSS (HR = 2.19, 95% CI = 1.07 to 4.48,  $P = .03$ ) ([Figure 6, E and F](#)). In this cohort, having early-stage (I-II), ER-positive, or non-TNBC tumors was associated with better survival outcomes ([Supplementary Figure 7, A-F](#), available online). Moreover, having NDRG1-high-expressing advanced-stage breast tumor was associated with reduced OS and BCSS relative to NDRG1-low-expressing advanced-stage tumors ( $P < .001$ ; [Supplementary Figure 7, A and B](#), available online). On multivariable analysis, NDRG1-high expression was

KD1 = 31.8 [14.46]; KD2 = 47.6 [20.82] days) and MDA-IBC3 (Ctl = 41 [8.42]; KD1 = 54.6 [10] days) xenografts. Horizontal lines indicate mean.  $P$  value from 2-sided  $t$  tests. D) Hematoxylin and eosin (HE) staining and immunostaining (for total and phosphorylated NDRG1 [NDRG1\_pT346]) of SUM149 xenografts. Arrowheads point to metaplastic squamous cell features in NDRG1 control cells. Scale bar = 100  $\mu$ m. E) HE and immunostaining (for total NDRG1 and NDRG1\_pT346) of MDA-IBC3-derived tumors. Scale bar = 100  $\mu$ m. F) Images of whole brains showing metastases labeled with red fluorescence protein. Panels below show HE staining of metastatic outgrowth in the brain. Scale bar = 200  $\mu$ m. Panels below immunostaining for total NDRG1 and NDRG1\_pT346. Scale bar = 100  $\mu$ m. G) Incidence of brain metastases after tail-vein injection of MDA-IBC3 control or NDRG1-silenced cells.  $P$  value from 2-sided Fisher's exact test. H) Quantification of brain metastasis burden in lesions generated from NDRG1 control and silenced MDA-IBC3 cells. Horizontal lines indicate mean and error bars indicate SD.  $P$  value from 2-sided Mann-Whitney test. I) Number of brain metastases per mouse, calculated as number of red fluorescence protein (RFP)-positive spots in the brain of each mouse. Horizontal lines indicate mean and error bars indicate SD and  $P$  value from 2-sided unpaired  $t$  test. HE = hematoxylin and eosin; OE = overexpression.

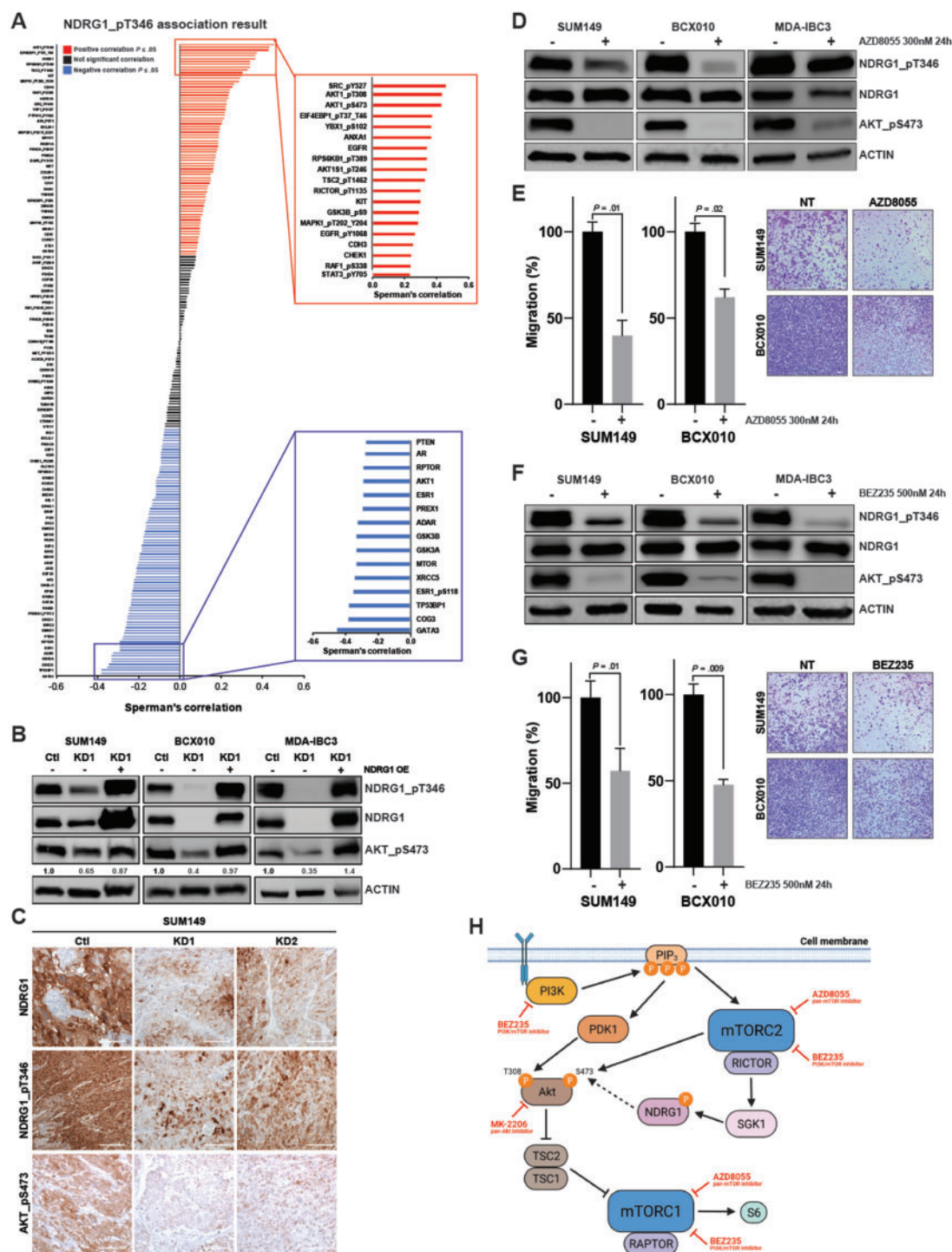


**Figure 5.** NDRG1 regulation of AKT signaling in aggressive breast cancer cells. **A**) Analysis of proteomic data from The Cancer Genome Atlas (TCGA) dataset shows correlations between phosphorylated NDRG1 (NDRG1\_pT346) expression and proteins in the mTOR-AKT pathway. In total 224 proteins are shown, and highlighted on the boxes on the right are the top positive or negative correlations. **B**) Immunoblotting for total NDRG1, NDRG1\_pT346, and phosphorylated AKT (AKT\_pS473) after overexpression of NDRG1 in the silenced cells. Actin was used as internal control. Quantification of AKT-pS473 is shown. **C**) Immunostaining of total NDRG1, NDRG1\_pT346, and AKT\_pS473 in SUM149-derived xenografts. Scale bar = 100  $\mu$ m. **D**) Immunoblotting for total NDRG1, NDRG1\_pT346, and pAKT\_S473 and **E**) quantification of migration after cells were treated with the dual mTOR inhibitor AZD8055 (300 nM for 24 hours). Bar graphs indicate mean and error bars indicate SD, calculated after 3 independent experiments; P values from 2-sided t tests. Scale bar = 200  $\mu$ m. **F**) Immunoblotting for total NDRG1, NDRG1\_pT346, and pAKT\_S473 and **G**) quantification of migration after cells were treated with the dual PI3K-mTOR inhibitor BEZ235 (500 nM for 24 hours). Bar graphs indicate mean and error bars indicate SD, calculated after 3 independent experiments; P values from 2-sided t tests. Scale bar = 200  $\mu$ m. **H**) Proposed mechanism of actions of NDRG1. PI3K phosphorylates PIP3, which in turn activates PDK1 and mTORC2. AKT is phosphorylated at T308 by PDK1 and at S473 by mTORC2; after both phosphorylations, AKT activates mTORC1. mTORC2 activates SGK1, which phosphorylates NDRG1, and that, at least in part, affects phospho-AKT status. AKT = AKT serine/threonine kinase; Ctl = shRNA control; KD1 = knockdown variant 1; KD2 = knockdown variant 2; mTOR = mechanistic target of rapamycin kinase; mTORC1 = mTOR complex 1; mTORC2 = mTOR Complex 2; NDRG1 = N-Myc downstream regulated 1; OE = overexpression; PDK1 = pyruvate dehydrogenase kinase 1; PI3K = phosphatidylinositol-4,5-bisphosphate 3-kinase; RAPTOR = regulatory-associated protein of mTOR complex 1; RICTOR = RPTOR-independent companion of mTOR complex 2; SD = standard deviation; SGK1 = serum/glucocorticoid regulated kinase 1; TSC = TSC complex subunit.



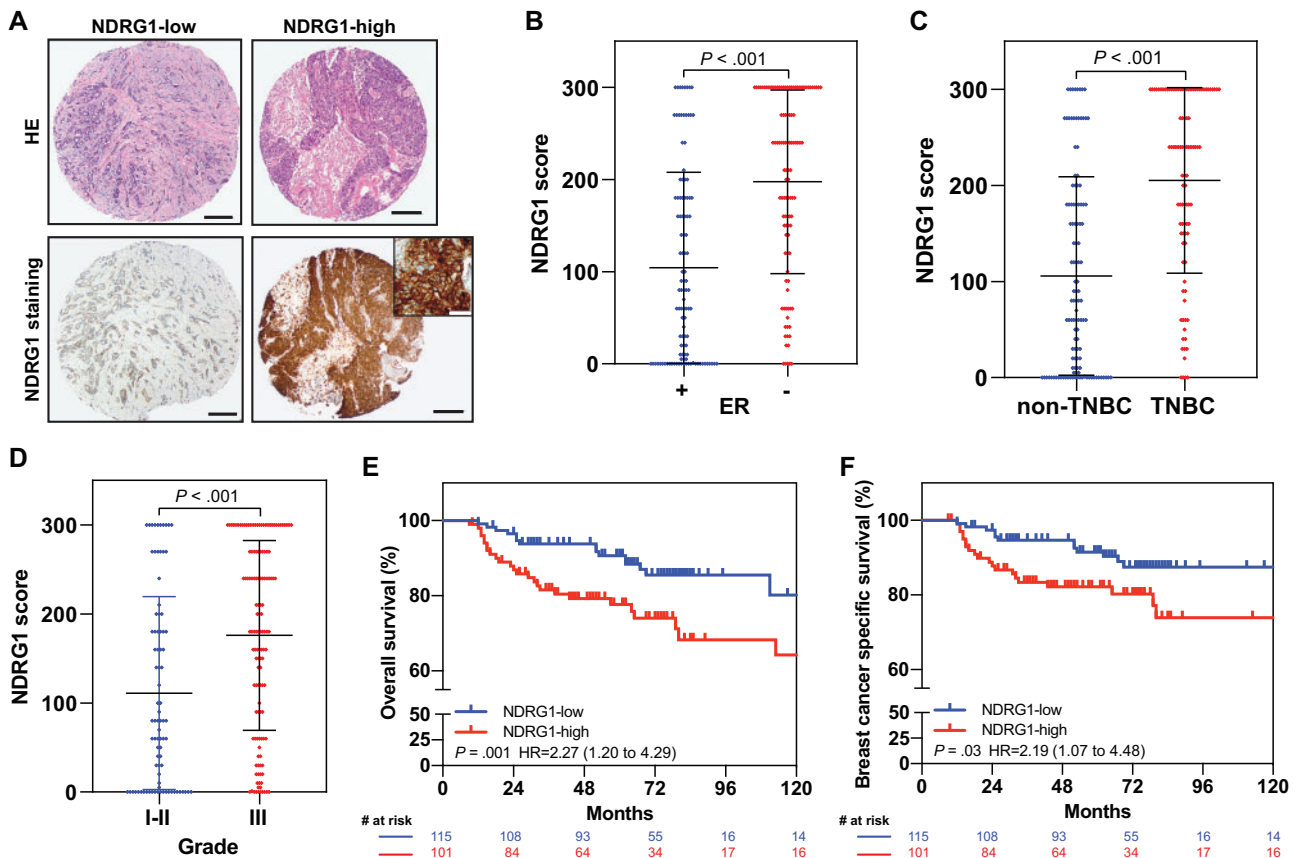


**Figure 6.** Prognostic significance of NDRG1 in patients with breast cancer. **A)** Representative photomicrographs of NDRG1 expression in tissue microarrays from breast cancer patients; left, an invasive breast carcinoma with weak and focal staining for NDRG1; right, another invasive breast carcinoma with strong and diffuse staining for NDRG1. Scale bar = 200  $\mu$ m. Inset, high-magnification photomicrograph shows cytoplasmic and membranous NDRG1 staining in tumor cells. Scale bar = 50  $\mu$ m. NDRG1 expression according to **(B)** estrogen receptor, **(C)** triple-negative breast cancer (TNBC), and **(D)** grade status. Horizontal lines indicate medians and error bars indicate SD; P values from 2-sided Mann-Whitney tests. Kaplan-Meier estimates of **(E)** overall survival and **(F)** breast cancer-specific survival according to NDRG1 expression. P values from log-rank tests, and the hazard ratio with 95% confidence interval (95% CI) is shown. ER = estrogen receptor; HR = hazard ratio.

found to be an independent predictor of OS (HR = 2.17, 95% CI = 1.10 to 4.30,  $P = .03$ ) and BCSS (HR = 2.27, 95% CI = 1.05 to 4.92,  $P = .04$ ) (Table 2). Collectively, these findings demonstrate that NDRG1 is an independent predictor of poor outcome in breast cancer and suggest that NDRG1 is a critical contributor to the aggressiveness of breast tumors.

## Discussion

Although NDRG1 has been defined as a metastasis suppressor, increasing evidence demonstrates that it also functions as a promoter of tumorigenesis and metastasis in some cancer types. In this article, we report 1) NDRG1 correlated positively with poor clinical outcomes and with tumor traits that are frequently associated with aggressive phenotypes, 2) NDRG1 depletion in aggressive breast cancer cells reduced invasion and migration capacity and reduced tumor-initiating cell subpopulation, 3) NDRG1 is required for primary tumor growth and brain metastatic colonization in mouse models, 4) NDRG1-high protein expression predicts poor survival outcomes independently of other known prognostic variables, and 5) the tumor-promoting effect of NDRG1 is mediated through activation of mTOR-AKT signaling.

NDRG1 is known to be activated in the presence of cellular stress conditions, such as hypoxia, and is involved in resistance

to chemotherapy (31-35). In breast cancer, NDRG1 is widely described as suppressing tumorigenesis and metastasis by inhibition of proliferation and invasion of breast cancer cells (23-25). However, NDRG1 has also been associated with worse outcome and promotion of aggressiveness and tumorigenesis in breast cancer (36-38). We recently showed that NDRG1 was independently correlated with reduced OS and disease-specific survival in patients with inflammatory breast cancer (21). These observations suggest that NDRG1 has a context-dependent function in breast cancers. Indeed, many studies that described NDRG1 as a metastasis suppressor in breast cancer used ER-positive, less aggressive breast cancer cell lines such as MCF-7 (39-41). In the current study, we showed that NDRG1 functions as a promoter of tumor growth and brain metastasis in ER-negative, aggressive breast cancers. Indeed, analysis of multiple independent datasets indicated NDRG1 is statistically significantly higher in ER-negative tumors, aggressive molecular subtypes, and high-grade tumors; and patients with NDRG1-high-expressing tumors had worse survival outcomes. We confirmed these results by using several different approaches. First, we evaluated TMAs containing breast cancer xenografts and PDX tumors and found that NDRG1 was highly expressed in ER-negative and TNBC tumors. Second, we conducted in vitro and in vivo experiments using ER-negative, aggressive breast cancer cell lines and found that NDRG1 depletion reduced colony

**Table 1.** Clinicopathological characteristics of tumor samples from 216 patients with breast cancer according to NDRG1 expression

Variable	NDRG1-low (n = 115)	NDRG1-high (n = 101)	P
Age			
Mean (SD), y	54.74 (11.55)	55.72 (13.61)	.57 <sup>a</sup>
Age group, No. (%)			
≤ 55 y	62 (53.9)	51 (50.5)	.62 <sup>b</sup>
>55 y	53 (46.1)	50 (49.5)	
Race, no. (%)			
Black	12 (10.4)	25 (24.8)	.006 <sup>b</sup>
Hispanic	23 (20)	10 (9.9)	
Other	5 (4.3)	9 (8.9)	
White	75 (65.2)	57 (56.4)	
Pathological disease stage, No. (%)			
I	43 (37.7)	41 (41.8)	.81 <sup>c</sup>
II	43 (37.7)	32 (32.7)	
III	25 (21.9)	21 (21.4)	
IV	3 (2.6)	4 (4.1)	
Tumor grade, No. (%)			
1-2	58 (50.4)	27 (26.7)	<.001 <sup>b</sup>
3	57 (49.6)	74 (73.3)	
Hormone receptor, No. (%)			
Negative	38 (33)	69 (68.3)	<.001 <sup>b</sup>
Positive	77 (67)	32 (31.7)	
Estrogen receptor, No. (%)			
Negative	38 (33)	69 (68.3)	<.001 <sup>b</sup>
Positive	77 (67)	32 (31.7)	
Progesterone receptor, No. (%)			
Negative	48 (41.7)	82 (81.2)	<.001 <sup>b</sup>
Positive	67 (58.3)	19 (18.8)	
HER2, No. (%)			
Negative	90 (78.3)	85 (84.2)	.27 <sup>b</sup>
Positive	25 (21.7)	16 (15.8)	
Triple-negative breast cancer, No. (%)			
No	83 (72.2)	36 (35.6)	<.001 <sup>b</sup>
Yes	32 (27.8)	65 (64.4)	

<sup>a</sup>P value derived from 2-sided 2-sample t tests.<sup>b</sup>P values were derived from 2-sided  $\chi^2$  tests.<sup>c</sup>P value derived from 2-sided Fisher's exact test.

formation, migration, invasion, and tumor-initiating cells in vitro and primary tumor growth and brain metastasis colonization in vivo. Third, immunostaining of patient tumors demonstrated that NDRG1 is an independent prognostic factor for poorer OS and BCSS. These findings strongly support that NDRG1 is a critical contributor to tumor growth and metastasis in aggressive breast cancer. Of note, NDRG1, located in the 8q24 MYC amplicon locus, could be coamplified with MYC, a major driver of cancer aggressiveness and progression. Although our work suggests that NDRG1 is a driver of the oncogenic phenotypes we observed in aggressive breast cancers, we cannot exclude these phenotypes could also be a consequence of its coamplification with MYC. Little is known about whether the genes in the 8q24 locus that are coamplified with MYC (eg, NDRG1) have coordinated effects with MYC or act independently of MYC. Previous reports have shown that elevated NDRG1 expression is a more consistent biomarker of negative prognosis than the MYC oncogene (37).

Aggressive breast cancer subtypes, including HER2+ and TNBC, carry increased risks of developing brain metastasis. Our study showed the importance of NDRG1 as a mediator of brain metastasis development in 2 different mouse models. While this manuscript was being prepared, Berghoff et al. (42)

published findings that slow-cycling breast cancer cells are involved in the development of brain metastasis in breast cancer and that NDRG1 was highly expressed in those cells, corroborating our results. Similarly, this group found a negative correlation between NDRG1 expression and ER status, consistent with our work. However, we observed some discrepancy between their work and this study in the immunostaining results, which in part reflects differences in the patient populations and immunostaining pattern. For example, Berghoff et al. (42) considered only membranous staining of NDRG1, whereas our study included both cytoplasmic and membranous staining because NDRG1 labels predominantly tumor cells at the cytoplasm or membrane. Indeed, our immunostaining showed 41.2% cytoplasmic, 9.3% membranous, and 29.6% both.

The presence of hypoxic and necrotic areas is associated with aggressive, fast-growing tumors, and the presence of necrosis is a prognostic factor for breast cancer recurrence and poor outcome (28,29). NDRG1 is known to localize in hypoxic areas adjacent to necrosis. In hepatocellular carcinoma cells, NDRG1 expression was associated with hypoxia-related resistance to doxorubicin, and silencing of NDRG1 increased the sensitivity of hypoxic cells to treatment (31,35,43,44). In our study, we observed that xenografts from NDRG1-silenced SUM149 cells

Table 2. Univariate and multivariable Cox regression analysis of OS and BCSS from 216 patients with breast cancer

Covariate	Univariate analysis			Multivariable analysis		
	OS		BSCC	OS		BCSS
	HR (95% CI)	P <sup>a</sup>	HR (95% CI)	HR (95% CI)	P <sup>b</sup>	HR (95% CI)
Age group						
≤55 years	1.00 (Referent)		1.00 (Referent)			
>55 years	0.99 (0.54 to 1.82)	.97	0.62 (0.30 to 1.27)			
Pathological disease stage						
I	1.00 (Referent)		1.00 (Referent)	1.00 (Referent)		1.00 (Referent)
II	2.36 (0.88 to 6.29)	.09	10.39 (1.32 to 82.05)	2.41 (0.90 to 6.43)	.08	10.64 (1.35 to 84.15)
III	6.64 (2.58 to 17.10)	<.001	34.81 (4.59 to 263.84)	9.34 (3.57 to 24.47)	<.001	48.73 (6.35 to 347.14)
IV	29.85 (9.33 to 85.47)	<.001	162.61 (19.24 to 1374.60)	38.02 (11.44 to 126.37)	<.001	208.32 (24.00 to 1808.31)
Grade						
1-2	1.00 (Referent)		1.00 (Referent)			
3	4.20 (1.76 to 10.01)	.001	3.97 (1.53 to 10.33)			
Hormone receptor status						
Negative	1.00 (Referent)		1.00 (Referent)	1.00 (Referent)		1.00 (Referent)
Positive	0.40 (0.20 to 0.79)	.008	0.48 (0.23 to 1.00)	0.32 (0.15 to 0.69)	.004	0.36 (0.16 to 0.82)
Estrogen receptor status						
Negative	1.00 (Referent)		1.00 (Referent)			
Positive	0.40 (0.20 to 0.79)	.008	0.48 (0.23 to 1.00)			
Progesterone receptor status						
Negative	1.00 (Referent)		1.00 (Referent)			
Positive	0.29 (0.13 to 0.66)	.003	0.31 (0.13 to 0.76)			
HER2 status						
Negative	1.00 (Referent)		1.00 (Referent)			
Positive	0.43 (0.13 to 1.39)	.16	0.16 (0.02 to 1.19)			
Triple-negative breast cancer status						
Negative	1.00 (Referent)		1.00 (Referent)			
Positive	2.29 (1.19 to 4.41)	.01	2.10 (1.02 to 4.32)			
NDRG1						
Low	1.00 (Referent)		1.00 (Referent)	1.00 (Referent)		1.00 (Referent)
High	2.27 (1.20 to 4.29)	.01	2.19 (1.07 to 4.48)	2.17 (1.10 to 4.30)	.03	2.27 (1.05 to 4.92)

<sup>a</sup>P values are based on 2-sided test from univariate Cox regression model. BCSS = breast cancer specific survival; CI = confidence interval; HR = hazard ratio, OS = overall survival.

<sup>b</sup>P values are based on 2-sided test from multivariable Cox regression model.

showed statistically significantly smaller necrotic areas. We further observed a statistically significant positive correlation between NDRG1 expression and percentage of necrosis in tumors in the TMAs of PDXs and xenograft tumors, further supporting our findings that NDRG1 is associated with aggressive phenotypic traits.

In conclusion, our results underscore the importance of NDRG1 in tumor growth and metastasis of aggressive breast cancer. We further found NDRG1 to be an independent predictor of poor clinical outcome in patients with breast cancer. These results suggest that NDRG1 may serve as a therapeutic target and prognostic biomarker in aggressive breast cancers.

## Funding

This study was supported in part by the following grants: American Cancer Society Research Scholar grant (RSG-19-126-01 to BGD), Susan G. Komen Career Catalyst Research Grant (CCR16377813 to BGD), Startup and Institutional Research Grants from MD Anderson, The Morgan Welch Inflammatory Breast Cancer Boot Walk Fund (to ESV), and the NCI/NIH Cancer Center Support (Core) Grant P30 CA016672 and the NCI's Research Specialist Award 1 R50 CA243707-01A1 to The University of Texas MD Anderson Cancer Center.

## Notes

**Role of the funder:** The study sponsors had no role in the design of the study; the collection, analysis, or interpretation of the data; the writing of the manuscript; or the decision to submit the manuscript for publication.

**Disclosures:** The authors declare no conflicts of interest.

**Author contributions:** Conceptualization: ESV and BGD. Data curation: ESV, XH, BLE, RL, LH and BGD. Formal Analysis: ESV, BLE, LH, ECY, JS, SK and BGD. Funding acquisition: BGD. Investigation: ESV, XH, BLE, LH, ECY, JS, SK and BGD. Methodology: ESV, XH, LH, ECY, JS and BGD. Resources: YG, SL, SP, NTU, WAW, and DT. Writing—original draft: ESV, BGD. Writing—review & editing: ESV, XH, BLE, LH, JS, SL, NTU, SK, DT, WAW, BGD.

**Prior presentations:** Part of this study was presented at San Antonio Breast Cancer Symposium (SABCS), 2019.

**Acknowledgements:** We thank Christine F. Wogan, MS, ELS, of MD Anderson's Division of Radiation Oncology for scientific editing and review of the manuscript and Carol M. Johnston from the Division of Surgery Histology Core at MD Anderson for her help with immunohistochemical staining.

## Data Availability

The data that support the findings of this study are available from the corresponding author (bgdebeb@mdanderson.org) upon reasonable request. Additional data are available as [supplementary material](#).

## References

- Achrol AS, Rennert RC, Anders C, et al. Brain metastases. *Nat Rev Dis Primers*. 2019;5(1):5.
- Nayak L, Lee EQ, Wen PY. Epidemiology of brain metastases. *Curr Oncol Rep*. 2012;14(1):48–54.
- Dawood S, Ueno NT, Valero V, et al. Incidence of and survival following brain metastases among women with inflammatory breast cancer. *Ann Oncol*. 2010; 21(12):2348–2355.
- Uemura MI, French JT, Hess KR, et al. Development of CNS metastases and survival in patients with inflammatory breast cancer. *Cancer*. 2018;124(11): 2299–2305.
- Warren LE, Guo H, Regan MM, et al. Inflammatory breast cancer and development of brain metastases: risk factors and outcomes. *Breast Cancer Res Treat*. 2015;151(1):225–232.
- Oehrlich NE, Spinelli LM, Papendorf F, et al. Clinical outcome of brain metastases differs significantly among breast cancer subtypes. *Oncol Lett*. 2017; 14(1):194–200.
- Ostrom QT, Wright CH, Barnholtz-Sloan JS. Brain metastases: epidemiology. *Handb Clin Neurol*. 2018;149:27–42.
- Debeb BG, Lacerda L, Anfossi S, et al. miR-141-mediated regulation of brain metastasis from breast cancer. *J Natl Cancer Inst*. 2016;108(8):djw026.
- Hu X, Villodre ES, Woodward WA, et al. Modeling brain metastasis via tail-vein injection of inflammatory breast cancer cells. *J Vis Exp*. 2021;(168). doi: 10.3791/62249(168).
- Fukumura K, Malgouwar PB, Fischer GM, et al. Multi-omic molecular profiling reveals potentially targetable abnormalities shared across multiple histologies of brain metastasis. *Acta Neuropathol*. 2021;141(2):303–321.
- Smith DL, Debek BG, Diagaradjane P, et al. Prophylactic cranial irradiation reduces the incidence of brain metastasis in a mouse model of metastatic, HER2-positive breast cancer. *Genes Cancer*. 2021;12:28–38.
- Smith DL, Debek BG, Thames HD, et al. Computational modeling of micrometastatic breast cancer radiation dose response. *Int J Radiat Oncol Biol Phys*. 2016;96(1):179–187.
- Angst E, Dawson DW, Stroka D, et al. N-myc downstream regulated gene-1 expression correlates with reduced pancreatic cancer growth and increased apoptosis in vitro and in vivo. *Surgery*. 2011;149(5):614–624.
- Chang X, Xu X, Ma J, et al. NDRG1 expression is related to the progression and prognosis of gastric cancer patients through modulating proliferation, invasion and cell cycle of gastric cancer cells. *Mol Biol Rep*. 2014;41(9):6215–6223.
- Jin R, Liu W, Menezes S, et al. The metastasis suppressor NDRG1 modulates the phosphorylation and nuclear translocation of beta-catenin through mechanisms involving FRAT1 and PAK4. *J Cell Sci*. 2014;127(Pt 14):3116–3130.
- Mi L, Zhu F, Yang X, et al. The metastatic suppressor NDRG1 inhibits EMT, migration and invasion through interaction and promotion of caveolin-1 ubiquitylation in human colorectal cancer cells. *Oncogene*. 2017;36(30):4323–4335.
- Cheng J, Xie HY, Xu X, et al. NDRG1 as a biomarker for metastasis, recurrence and of poor prognosis in hepatocellular carcinoma. *Cancer Lett*. 2011;310(1): 35–45.
- Li A, Zhu X, Wang C, et al. Upregulation of NDRG1 predicts poor outcome and facilitates disease progression by influencing the EMT process in bladder cancer. *Sci Rep*. 2019;9(1):5166.
- Liu Y, Wang D, Li Y, et al. Long noncoding RNA CCAT2 promotes hepatocellular carcinoma proliferation and metastasis through up-regulation of NDRG1. *Exp Cell Res*. 2019;379(1):19–29.
- Nishio S, Ushijima K, Tsuda N, et al. Cap43/NDRG1/Drg-1 is a molecular target for angiogenesis and a prognostic indicator in cervical adenocarcinoma. *Cancer Lett*. 2008;264(1):36–43.
- Villodre ES, Gong Y, Hu X, et al. NDRG1 expression is an independent prognostic factor in inflammatory breast cancer. *Cancers (Basel)*. 2020;12(12):3711.
- Yan X, Chua MS, Sun H, et al. N-Myc down-regulated gene 1 mediates proliferation, invasion, and apoptosis of hepatocellular carcinoma cells. *Cancer Lett*. 2008;262(1):133–142.
- Bandyopadhyay S, Pai SK, Hirota S, et al. Role of the putative tumor metastasis suppressor gene Drg-1 in breast cancer progression. *Oncogene*. 2004;23(33): 5675–5681.
- Godbole M, Togar T, Patel K, et al. Up-regulation of the kinase gene SGK1 by progesterone activates the AP-1-NDRG1 axis in both PR-positive and -negative breast cancer cells. *J Biol Chem*. 2018;293(50):19263–19276.
- Han LL, Hou L, Zhou MJ, et al. Aberrant NDRG1 methylation associated with its decreased expression and clinicopathological significance in breast cancer. *J Biomed Sci*. 2013;20(1):52.
- Tian S, Wang X, Proud CG. Oncogenic MNK signalling regulates the metastasis suppressor NDRG1. *Oncotarget*. 2017;8(28):46121–46135.
- Ciriello G, Gatza ML, Beck AH, et al.; TCGA Research Network. Comprehensive molecular portraits of invasive lobular breast cancer. *Cell*. 2015;163(2):506–519.
- Gilchrist KW, Gray R, Fowble B, et al. Tumor necrosis is a prognostic predictor for early recurrence and death in lymph node-positive breast cancer: a 10-year follow-up study of 728 Eastern Cooperative Oncology Group patients. *J Clin Oncol*. 1993;11(10):1929–1935.
- Tata A, Woolman M, Ventura M, et al. Rapid detection of necrosis in breast cancer with desorption electrospray ionization mass spectrometry. *Sci Rep*. 2016;6:35374.
- Hennessy BT, Krishnamurthy S, Giordano S, et al. Squamous cell carcinoma of the breast. *J Clin Oncol*. 2005;23(31):7827–7835.

31. Cangul H. Hypoxia upregulates the expression of the NDRG1 gene leading to its overexpression in various human cancers. *BMC Genet.* 2004;5:27.
32. Chiang CT, Demetriou AN, Ung N, et al. mTORC2 contributes to the metabolic reprogramming in EGFR tyrosine-kinase inhibitor resistant cells in non-small cell lung cancer. *Cancer Lett.* 2018;434:152–159.
33. Fotovati A, Abu-Ali S, Kage M, et al. N-myc downstream-regulated gene 1 (NDRG1) a differentiation marker of human breast cancer. *Pathol Oncol Res.* 2011;17(3):525–533.
34. Lee GY, Chun YS, Shin HW, et al. Potential role of the N-MYC downstream-regulated gene family in reprogramming cancer metabolism under hypoxia. *Oncotarget.* 2016;7(35):57442–57451.
35. Weiler M, Blaes J, Pusch S, et al. mTOR target NDRG1 confers MGMT-dependent resistance to alkylating chemotherapy. *Proc Natl Acad Sci USA.* 2014;111(1):409–414.
36. Mao XY, Fan CF, Wei J, et al. Increased N-myc downstream-regulated gene 1 expression is associated with breast atypia-to-carcinoma progression. *Tumour Biol.* 2011;32(6):1271–1276.
37. Sevinsky CJ, Khan F, Kokabee L, et al. NDRG1 regulates neutral lipid metabolism in breast cancer cells. *Breast Cancer Res.* 2018;20(1):55.
38. Nagai MA, Gerhard R, Fregnani JH, et al. Prognostic value of NDRG1 and SPARC protein expression in breast cancer patients. *Breast Cancer Res Treat.* 2011;126(1):1–14.
39. Chiang KC, Yeh CN, Chung LC, et al. WNT-1 inducible signaling pathway protein-1 enhances growth and tumorigenesis in human breast cancer. *Sci Rep.* 2015;5:8686.
40. Lai LC, Su YY, Chen KC, et al. Down-regulation of NDRG1 promotes migration of cancer cells during reoxygenation. *PLoS One.* 2011;6(8):e24375.
41. Liu W, Xing F, Iizumi-Gairani M, et al. N-myc downstream regulated gene 1 modulates Wnt-beta-catenin signalling and pleiotropically suppresses metastasis. *EMBO Mol Med.* 2012;4(2):93–108.
42. Berghoff AS, Liao Y, Karreman MA, et al. Identification and characterization of cancer cells that initiate metastases to the brain and other organs. *Mol Cancer Res.* 2021;19(4):688–701.
43. Jung EU, Yoon JH, Lee YJ, et al. Hypoxia and retinoic acid-inducible NDRG1 expression is responsible for doxorubicin and retinoic acid resistance in hepatocellular carcinoma cells. *Cancer Lett.* 2010;298(1):9–15.
44. Tomes L, Emberley E, Niu Y, et al. Necrosis and hypoxia in invasive breast carcinoma. *Breast Cancer Res Treat.* 2003;81(1):61–69.